JOURNAL OF SOLID STATE CHEMISTRY **121,** 372–378 (1996)
ARTICLE NO. 0050

Characterization by X-Ray Absorption, X-Ray Powder Diffraction, and Magnetic Susceptibility of Cu–Zn–Co–Al–Containing Hydroxycarbonates, Oxycarbonates, Oxides, and Their Products of Reduction

Piero Porta,[1] Simone Morpurgo, and Ida Pettiti

Centro del CNR su 'Struttura ed Attività Catalitica di Sistemi di Ossidi' (SACSO), c/o Dipartimento di Chimica, Università 'La Sapienza', Piazzale Aldo Moro 5, 00185 Rome, Italy

Received June 1, 1995; in revised form October 16, 1995; accepted October 17, 1995

Copper-zinc-cobalt-aluminium-containing crystalline hydroxycarbonates having hydrotalcite structure have been prepared by coprecipitation. X-ray powder diffraction (XRPD), magnetic susceptibility, and extended X-ray absorption fine structure (EXAFS) indicate that Cu^{2+}, Zn^{2+}, and Co^{2+} are present in an octahedral environment. Calcination of the hydroxycarbonates at 723 K produces quasi-amorphous oxycarbonates where Cu^{2+} and Co^{2+} still retain octahedral coordination and cobalt is almost completely oxidized to Co^{3+}. The coordination of Zn^{2+}, at this stage, is intermediate between the octahedral one of the precursors and the tetrahedral one of ZnO and Zn-based spinels. Further calcination at 973 K produces a mixture of crystalline oxides such as CuO, ZnO, $CuAl_2O_4$, $ZnAl_2O_4$, and $ZnCo_2O_4$. EXAFS analysis of these samples indicates that copper is mainly in a fourfold coordination (although two longer Cu–O distances are also detected), zinc is tetrahedral, and cobalt (as Co^{3+}) is essentially octahedral. EXAFS and XANES investigations performed after *in situ* reduction (10% H_2/N_2, at 523 and 623 K) on the oxycarbonates and oxides reveal that the total $Cu^{2+} \rightarrow Cu^0$ reduction occurs only at 623 K in both series of samples, Co^{3+} is reduced to Co^{2+} only at 623 K in the oxycarbonates, and Zn^{2+} is never reduced.

INTRODUCTION

Methanol, higher alcohols, and hydrocarbons can conveniently be synthesized through the syngas reaction performed by heterogeneous catalysis (1, 2). Several materials have been studied to this purpose and, among them, copper-based mixed oxide systems represented as CuO/ZnO/M_2O_3 (where M = Al, Cr, Ga) allow the reaction to be performed at relatively low temperature (<573 K) and pressure (50–100 atm). It has also been found that the addition of cobalt to CuO/ZnO/M_2O_3 materials results in a better selectivity toward the formation of higher alcohols and hydrocarbons with respect to methanol (3–6). However, there is no general agreement about the nature of the catalytically active cobalt-containing phase, and it is still questioned whether it consists of metallic cobalt (pure or alloyed with Cu°) (4, 5), or of a multicomponent spinel phase containing either Co^{2+} and Co^{3+} (6). The nature of catalytically active copper has also long been debated (7, 8).

Homogeneous and well-interdispersed mixed oxide systems, whose catalytic activity results from a cooperative effect (also referred to as "chemical promotion") (7) between their components, are generally obtained by calcination of precursors, preferably containing all the metal cations randomly distributed within the same phase (7–11). A class of compounds which can successfully be employed as precursors are the layered double hydroxydes (LDHs or hydrotalcite-like structures) (12) corresponding to the following stoichiometric formula: $M_6^{2+}M_2^{3+}(OH)_{16}CO_3 \cdot 4H_2O$, where M^{2+} = Cu, Zn, Co, Ni, etc., and M^{3+} = Al, Cr, Fe. The synthesis of new quaternary Cu–Zn–Co–Al–based LDH precursors and their thermal decomposition, at first to amorphous, then to crystalline mixed oxides has been reported in a previous paper (13). This study has shown that the thermal decomposition of LDHs is a continuous process in which the step *precursors* → *amorphous oxides* is reversible. However, amorphous mixed oxides (which are the actual catalysts for syngas reaction) can not be characterized by X-ray powder diffraction. For this reason, the present analysis has been performed by EXAFS, which is sensitive to the local environment around the metal cations. The cation coordination, which is expected to undergo a continuous variation with calcination temperature, has been determined and compared for precursors, amorphous and crystalline mixed oxides and, finally, reduction products. The oxidation state of the metal

[1] To whom correspondence should be addressed.

0022-4596/96 $18.00

TABLE 1
Phases Detected by X-Ray Diffraction, Experimental Curie Constants (C_{exp}), Magnetic Moments (μ, in Bohr Magnetons μ_B), Weiss Temperatures (θ/K), Observed *Me*–O Distances (in Å), and Coordination Numbers (N)

Sample	Phases[a] (XRD)	C_{exp}	μ/μ_B	θ/K	Cu–O/N	Zn–O/N	Co–O/N
Co = 0							
Hydroxycarbonate	HT	0.42	1.83	0	1.95–6	2.06–6	
Oxycarbonate	am, T	0.31	1.57	73	1.93–6	1.96–6 (1.94–5, 2.07–1)[b]	
Oxide	T, Z, S				1.95–6 (1.93–4, 2.34–2)[b]	1.92–4	
Reduced oxycarbonate	Cu°				2.52–12	1.94–4	
Reduced oxide	Z, S, Cu°				2.53–12	1.94–4	
Co = 15							
Hydroxycarbonate	HT	1.19	3.09	0	1.95–5	2.08–6	2.07–6
Oxycarbonate	am, T	0.34	1.58	65	1.93–6	1.95–6 (1.92–5, 2.05–1.5)[b]	(1.84–6, 1.97–6)[b]
Oxide	T, S				(1.93–4, 2.34–2)[b]	1.92–4	(1.84–6, 1.97–6)[b]
Reduced oxycarbonate	Cu°				2.53–12	1.95–6 (1.90–4, 2.04–5)[b]	2.02–6
Reduced oxide	S, Cu°				2.53–12	1.91–4	(1.85–6, 1.98–6)[b]
Reference							
CuO					(1.94–4, 2.36–2)[b]		
Cu metal					2.53–12		
ZnO						1.95–4	
Co_3O_4							(1.86–6, 1.99–4)[b]

[a] HT, hydrotalcite; am, amorphous; T, tenorite; Z, zincite; S, spinel; Cu°, metallic copper.
[b] In the brackets, distances and coordination numbers obtained by a two-shell fit.

cations in the different materials have been evaluated by means of XANES and measurements of magnetic susceptibility. X-ray powder diffraction has been used for phase analysis.

EXPERIMENTAL

Hydroxycarbonate precursors were prepared by coprecipitation. A solution containing the metal nitrates in the desired stoichiometry was added under vigorous stirring to a $NaHCO_3$ solution at a constant temperature of 333 K. The slurry was aged for 4 h in the same conditions. The pH just after precipitation was 6.5–7.0, whereas the final one was 9.0–9.5. The precipitate, after washing with cold distilled water, was dried in an oven at 363 K. Elemental analysis has been performed by atomic absorption. The two samples studied in this work, hereafter labeled as Co = 0 and Co = 15, have, respectively, the following composition (at.%, with nominal values in brackets): Cu = 51.7 (52.5), Zn = 19.5 (22.5), Al = 28.8 (25.0); Cu = 41.4 (42.0), Zn = 15.4 (18.0), Co = 13.9 (15.0), Al = 29.3 (25.0). Precursors were calcined for 6 h at different temperatures (723 and 973 K).

XRPD patterns were taken with a Philips automated PW 1729 diffractometer equipped with an IBM PS2 computer for data acquisition and analysis (software APD-Philips) and an HP plotter. Scans were taken with a 2θ step size of 0.01° and using Cu$K\alpha_1$ (nickel-filtered) radiation. XRPD data for reference hydroxycarbonates and oxides were taken from Ref. (14). Table 1 reports the phases present for each precursor, calcined and reduced sample.

Magnetic susceptibilities were measured by the Gouy method over the temperature range 100–290 K and at different magnetic-field strengths. Correction was made for the diamagnetism of the samples.

X-ray absorption measurements were carried out over the Cu, Zn, and Co *K*-edges at the SERC Daresbury Synchrotron X-ray source (station 7.1) using a Si(111) double-crystal monochromator. Reference compounds (Cu, CuO, ZnO, CoO, Co_3O_4), precursors, and mixed oxides were deposited on a "Millipore" membrane from a C_2H_5OH suspension and the EXAFS spectra were collected at 77 K. Oxide samples were pressed into pellets and *in situ* treated by a flowing gas mixture H_2/N_2 (10% H_2) at 623 K, the EXAFS spectra being then collected at room temperature. Data were taken to 13 $Å^{-1}$, with collection times typically around 35 min. X-ray spectra were analyzed using the suite of programs available at Daresbury, including the conversion program EXCALIB, the normalization and background subtraction program EXBACK, and the curve-fitting and refinement program EXCURV92. The EXAFS function was obtained from EXBACK and transferred to EXCURV92 for fitting after weighting it by a k^2 factor. Within EXCURV92 the EXAFS spectra of reference compounds were fitted by allowing atom-specific parameters to refine within reasonable values; phase shift functions were provided directly from EXCURV92. The errors associated with refined parameters are ≈10% in the

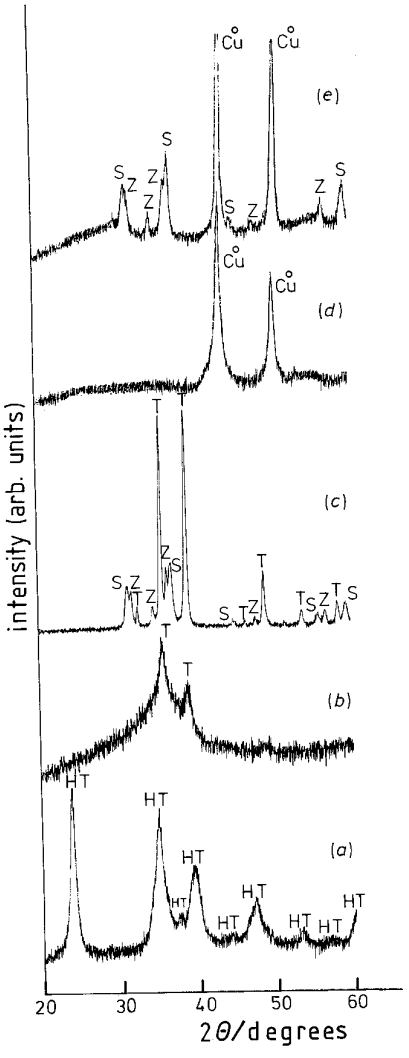

FIG. 1. XRPD patterns (Cu$K\alpha_1$) for the samples with Co = 0: (a) hydrotalcite; (b) oxycarbonate; (c) oxides; (d) reduced oxycarbonate; (e) reduced oxides. Symbols: HT, hydrotalcite; T, tenorite; Z, zincite; S, spinel: Cu^0, copper metal.

coordination numbers and Debye–Waller factors, and 0.02 Å in the coordination distances (15).

RESULTS AND DISCUSSION

Hydroxycarbonate Precursors

The LDH (hydrotalcite-like) structure consists of positively charged brucite-like layers, $[M_6^{2+}M_2^{3+}(OH)_{16}]^{2+}$, in which every cation is octahedrally surrounded by six OH groups (the octahedral units share edges and vertices), regularly alternating with hydrated negatively charged interlayers $(CO_3 \cdot 4H_2O)^{2-}$ (16). It may be recalled that the M–O distance within the hydrotalcite structure is 2.03 Å (17).

The XRPD patterns of the precursors Co = 0 and Co = 15 are reported in Figs. 1a and 2a, respectively. They show the typical trend of LDHs, in which the peaks spaced at regular 2θ intervals are originated by the reflections on the $(00l)$ planes. The sample Co = 0 displays a higher crystallinity than the Co = 15.

The oxidation state of copper and cobalt in the precursors could be determined by measurements of magnetic susceptibility. $1/\chi_m$ vs T plots (χ_m, molar magnetic susceptibility) obtained for the hydroxycarbonate precursors Co = 15 and Co = 0 are reported in Figs. 3a and 3b, respectively. In both cases the Curie–Weiss law, $\chi_m = C/(T + \theta)$, is obeyed, with a θ (Weiss temperature) value close to zero, indicating the lack of magnetic interactions between the paramagnetic ions (Cu^{2+} and Co^{2+}) and thus their random distribution within the brucite-like layers.

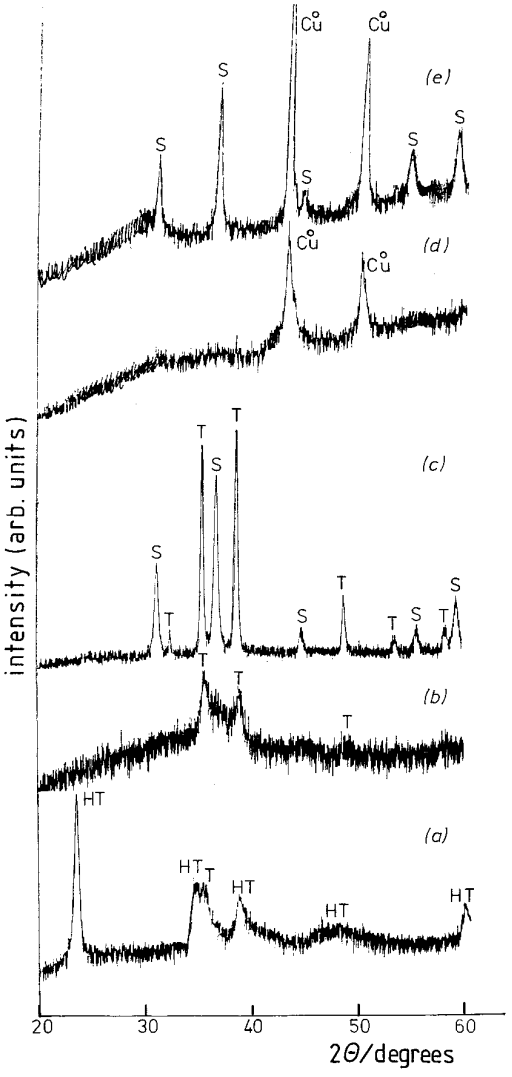

FIG. 2. XRPD patterns (Cu$K\alpha_1$) for the samples with Co = 15: (a) hydrotalcite; (b) oxycarbonate; (c) oxides; (d) reduced oxycarbonate; (e) reduced oxides. Symbols: HT, hydrotalcite; T, tenorite; Z, zincite; S, spinel; Cu^0, copper metal.

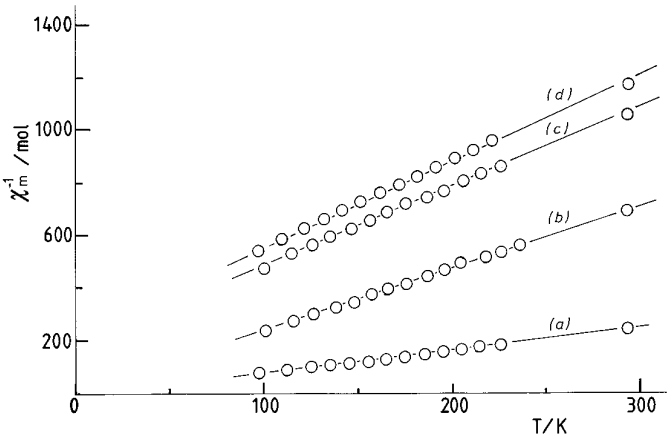

FIG. 3. Reciprocal molar magnetic susceptibility, $1/\chi_m$, vs T: (a) hydrotalcite with Co = 15; (b) cobalt-free hydrotalcite; (c) oxycarbonate with Co = 15; (d) cobalt-free oxycarbonate.

The experimental values of C and θ are reported in Table 1. The C value of 0.42 obtained for the sample Co = 0 yields an effective magnetic moment $\mu_{\text{eff}} = 2.828\sqrt{C} = 1.83\ \mu_B$ in agreement with the one expected for Cu^{2+} in octahedral symmetry (18). The oxidation state of cobalt in the sample Co = 15 could be calculated from the additivity law formula: $C = C_{Cu}X_{Cu} + C_{Co}X_{Co}$ (X is the molar fraction of a given cation with respect to the total amount of paramagnetic species). From $C = 1.19$ (experimental), $C_{Cu} = 0.42$ (taken from the sample Co = 0), and taking into account the sample composition, the value $C_{Co} = 3.48$ ($\mu_{\text{eff}} = 5.25\ \mu_B$) so obtained fairly agrees with that expected for Co^{2+} in octahedral coordination (19).

Figure 4 shows as an example the Fourier transforms (without phase shift correction) derived from the EXAFS spectra taken over the Cu, Zn, and Co K-edges of the sample Co = 15. The dominant peaks at ca. 1.7 and 2.8 Å, corresponding to the first and second scattering shells, reveal a qualitatively similar coordination for all cations. Fourier filtering, backtransform, and fitting of the first coordination shell showed (Table 1) that each cation is surrounded by six oxygens, with M–O distances of 1.95 Å for copper and in the range 2.06–2.08 Å for zinc and cobalt. The same results were obtained for the sample Co = 15.

Since the average M–O distance observed for the octahedrally coordinated cations in the pure hydrotalcite $[Mg_6Al_2(OH)_{16}CO_3 \cdot 4H_2O]$ structure is 2.03 Å (17), the values determined for Zn–O and Co–O bonds are satisfactory. The lower value of the Cu–O distance may be explained admitting a D_{4h} distortion of the copper sites (a shortening of the four planar bonds and a lengthening of the two apical ones), resulting in a shorter average distance. Note that in $Cu(OH)_2$ a very distorted octahedral coordination was found around copper (four planar Cu–O distances equal to 1.94 Å and two apical ones equal to 2.63 Å) (20). Having observed that a fitting of the experimental data based on a coordination number of four around copper was rather unsatisfactory, the result obtained with a sixfold coordination can be considered the most reliable.

The short Cu–O distance may also be explained by the presence of a strong covalent character (recall that the purely ionic octahedral Cu^{2+}–O bond is 2.11 Å) (21). It may be added that also in the Zn^{2+}–O and Co^{2+}–O bonds (observed values in the range 2.06–2.08 Å) some covalency is present since the purely ionic octahedral Zn^{2+}–O and Co^{2+}–O distances are 2.12 and 2.125 Å, respectively (21).

Oxycarbonates

As already discussed in a previous paper (13), the thermal decomposition of LDH materials occurs first by loss of crystallization water at $373 \leq T/K \leq 423$, then by continuous dehydration of the brucite-like layers at $423 \leq T/K \leq 673$ and formation of oxycarbonate compounds with the following reaction:

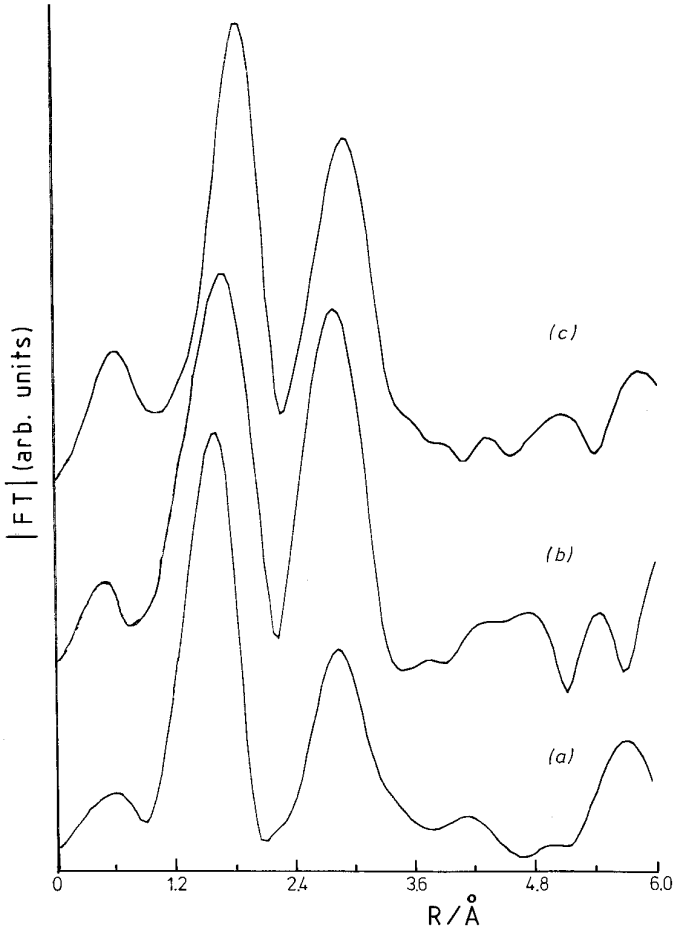

FIG. 4. EXAFS Fourier transform for hydrotalcite with Co = 15: (a) Cu K-edge; (b) Zn K-edge; (c) Co K-edge.

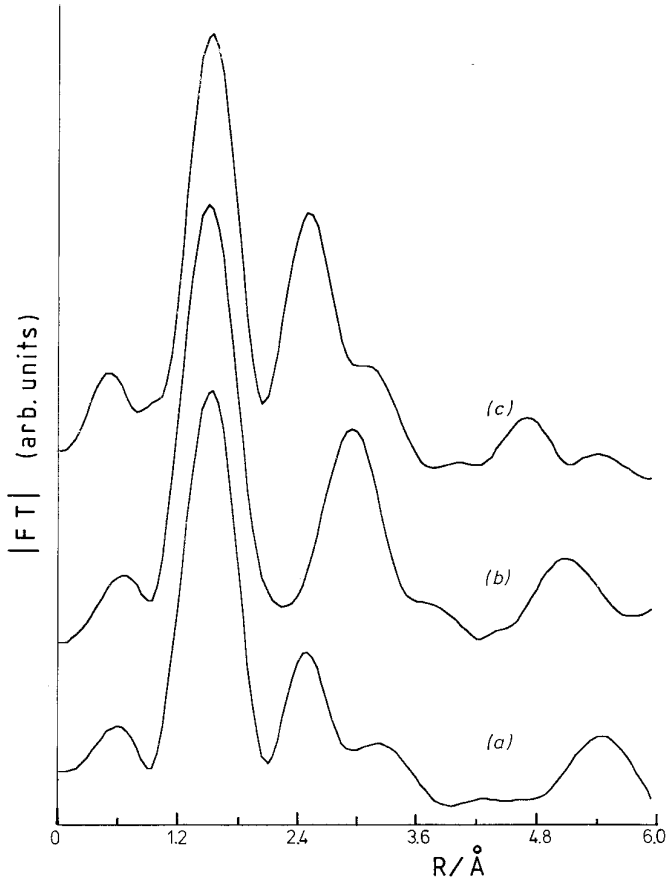

FIG. 5. EXAFS Fourier transform for oxycarbonate with Co = 15: (a) Cu *K*-edge; (b) Zn *K*-edge; (c) Co *K*-edge.

$$M_6^{2+}M_2^{3+}(OH)_{16}CO_3 \xrightarrow{423\text{–}673\ K} M_6^{2+}M_2^{3+}O_8CO_3 + 8H_2O.$$

The XRD patterns of the samples Co = 0 and Co = 15, calcined for 6 h at 723 K, are reported in Figs. 1b and 2b, respectively. In agreement with the results of the thermal analysis, the layered structure of the precursors is no more visible and the patterns show a quasi-amorphous structure with only two peaks at $2\theta \approx 35.7°$ and 38.9°, corresponding to the strongest lines of CuO (14b) and ascribed to the initial formation of small domains of tenorite. The magnetic results [Figs. 3c and 3d, Table 1] confirm the formation of the first nuclei of tenorite in the oxycarbonate materials since the observed value of the Weiss temperature θ (65–73 K) accounts for some antiferromagnetic interactions which are typical of CuO.

Figure 5 shows, as an example, the Fourier transforms calculated from the EXAFS spectra taken over the Cu, Zn, and Co *K*-edges of the sample Co = 15. For both Co = 0 and Co = 15 oxycarbonates, a qualitative analysis of the data revealed, for Cu^{2+}, a sixfold coordination similar to that observed in the precursors. Some difference with respect to precursors was instead observed for Zn^{2+}. Fourier filtering, subsequent backtransformations and fitting of the first coordination shell showed (see Table 1) that:

(i) the first coordination shell of Zn^{2+} is split into two peaks at fitted distances of 1.92–1.94 Å (with coordination number $N < 6$) and 2.05–2.07 Å ($1 < N < 2$). The deduced distances and the relative coordination numbers suggest that, at this stage of the decomposition process (T = 723 K), the coordination around zinc is probably undergoing a change from octahedral (found in the precursor) to tetrahedral.

(ii) For both samples the Cu–O and Zn–O distances are slightly shorter than those found in the precursors. This effect is indeed expected considering that dehydration produces stronger M–O bonds.

For the sample Co = 15, the fitting of the first coordination shell around cobalt revealed two Co–O distances of

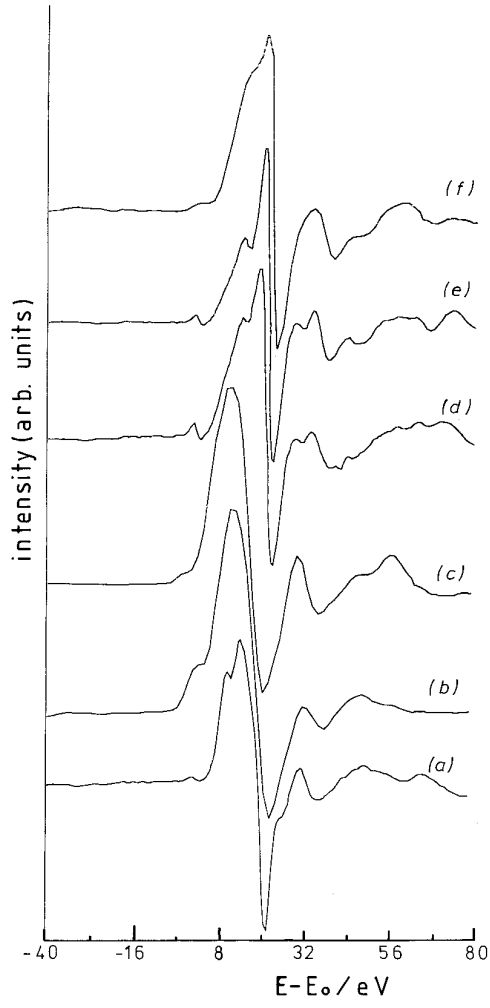

FIG. 6. First derivative of XANES on the Co *K*-edge of cobalt-containing materials: (a) hydrotalcite; (b) reduced oxycarbonate; (c) reference CoO; (d) oxycarbonate; (e) oxide; (f) reduced oxide.

1.84 and 1.97 Å (Table 1), whose values agree with those found for the model compound Co_3O_4 (Table 1) and indicate, as in Co_3O_4, the coexistence of Co^{2+} and Co^{3+} species.

The presence of the diamagnetic Co^{3+} species in the Co = 15 oxycarbonate is also drawn from magnetic results which strictly resemble [see Figs. 3c and 3d for comparison] those found for the Co = 0 oxycarbonate where the only paramagnetic species is Cu^{2+}. The observed value of C = 0.34, reported in Table 1, is comparable to that found for the Co = 0 oxycarbonate (C = 0.31) and shows that the contribution by cobalt to the paramagnetism of the sample is very low in the Co = 15 oxycarbonate. The amount of Co^{2+} (which has a value of $C = 3.48$, as derived from the Co = 15 hydroxycarbonate precursor, Table 1) is then negligible if the magnetic results are considered.

Qualitative information about the oxidation state of cobalt could also be obtained from XANES. It is widely known that the oxidation of a given element results in a shift of the relative XANES first derivative peak toward higher energies (22, 23). The XANES first derivatives obtained over the Co *K*-edge of the sample Co = 15 are shown in Fig. 6. The high-energy shift displayed by the oxycarbonate [curve d] with respect to the corresponding hydroxycarbonate [curve a], where cobalt is totally in the 2+ oxidation state, indicates that at least part of Co^{2+} contained in the precursor is oxidized to Co^{3+} in the oxycarbonate.

Oxides

As already discussed in a previous work (13) [for XRPD patterns see also Figs. 1c and 2c], precursor calcination at 973 K produces a mixture of crystalline oxides such as CuO (14b), ZnO (only present in the Co = 0 sample) (14c), $ZnAl_2O_4$ (14d), $CuAl_2O_4$ (14e), $CoAl_2O_4$ (very low amount detected) (14f), and $ZnCo_2O_4$ (14g).

EXAFS analysis performed over Cu, Zn, and Co *K*-edges revealed that (see Table 1):

(i) Both Co = 0 and Co = 15 samples contain Cu^{2+} in a distorted octahedral coordination, with Cu–O distances of 1.93 and 2.24 Å corresponding to those observed for CuO. Note that 1.93 Å is also the expected Cu–O bond distance for tetrahedral copper in the $CuAl_2O_4$ spinel.

(ii) Zn^{2+} is always found in tetrahedral coordination (as in ZnO, $ZnAl_2O_4$, and $ZnCo_2O_4$) with a Zn–O distance of 1.92 Å.

(iii) Cobalt is octahedrally coordinated, the value of Co–O = 1.84 Å being associated to the Co^{3+}–O distance in the $ZnCo_2O_4$ phase, and that at 1.97 Å corresponding to some Co^{2+} in $CoAl_2O_4$.

Reduced Samples

XRPD [Figs. 1d and 2d] and EXAFS (Table 1) performed on the oxycarbonates Co = 0 and Co = 15 reduced at 623 K showed that:

(i) Cu^{2+} is completely reduced to Cu^0 (14i). The Cu–Cu distance values (2.52 and 2.53 Å) agree with those found by us (Table 1) and quoted in the literature for metallic copper (24–26).

(ii) Zn^{2+} is not reduced and preserves the same Zn–O distance observed before reduction.

XANES first derivatives obtained over the Co *K*-edge for Co = 15 before and after reduction, respectively, are reported in Figs. 6d and 6b. The shift towards lower energies displayed after 623 K H_2/N_2 treatment can be accounted for a complete reduction of Co^{3+} (which is the predominant cobalt species in the starting oxycarbonate material) to Co^{2+}. The XANES first derivative obtained after reduction is additionally very similar to that of reference CoO [Fig. 6c].

Note that the fitted Co–O distance found by EXAFS analysis on the reduced Co = 15 oxycarbonate (2.02 Å, with $N = 6$) is close to that found in the LDH precursor (2.07 Å, $N = 6$) where Co^{2+} species are present in octahedral coordination.

As evidenced by XRPD [Figs 1e and 2e] and EXAFS analyses (Table 1), the H_2/N_2 treatment at 623 K of both mixed oxide samples (Co = 0 and Co = 15) results in a complete reduction of Cu^{2+} to Cu^0 whereas, as expected, Zn^{2+} contained in ZnO, $ZnAl_2O_4$, and $ZnCo_2O_4$ is not reduced at all. Co *K*-edge EXAFS (Table 1) and XANES [Fig. 6f] performed on the sample Co = 15 showed that Co^{3+} contained in the stable $ZnCo_2O_4$ spinel is not reduced to Co^{2+}, in contrast to what was observed after reducing treatment of the corresponding oxycarbonate sample.

The higher reducibility of oxycarbonates with respect to oxides is likely to be acsribed to the amorphous and layered nature of the oxycarbonates which allows higher diffusion of hydrogen.

CONCLUSIONS

The use of XRPD, magnetic susceptibility, and XAS complementary techniques has evidenced the following points:

(i) Hydroxycarbonate precursors are pure LDH materials containing all the elements (Cu^{2+}, Zn^{2+}, Co^{2+}, and Al^{3+}) in octahedral coordination. The absence of antiferromagnetic interactions indicates that the paramagnetic Cu^{2+} and Co^{2+} species are randomly distributed within the hydroxide framework. A certain degree of covalency, much stronger for copper, exists in the M^{2+}–OH bonds.

(ii) Precursor calcination at 723 K results in the formation of amorphous oxycarbonates, with partial segregation of CuO. Copper and cobalt are still found in roughly octahedral sites whereas zinc undergoes a change from octahedral to tetrahedral coordination. Co^{2+} is almost completely oxidized to Co^{3+}.

(iii) Precursor calcination at 973 K produces crystalline oxide mixtures containing CuO, ZnO, and spinel-like phases. Copper is mainly in a distorted octahedral symmetry, zinc is tetrahedrally coordinated, and cobalt (essentially as Co^{3+}) is in the octahedral sites of the $ZnCo_2O_4$ spinel.

(iv) After reduction at 623 K of oxycarbonates, Cu^{2+} and Co^{3+} are totally transformed to Cu^0 and Co^{2+}, respectively, whereas Zn^{2+} is not reduced. The reduction at 623 K of oxides leads to formation of metallic copper, essentially from tenorite, whereas the highly stable and crystalline spinel phases, namely $CuAl_2O_4$ and $ZnCo_2O_4$, are more resistant to reduction and the Cu^{2+} and Co^{3+} species contained in the spinels are unreduced.

REFERENCES

1. G. Natta, *in* "Catalysis" (P. H. Emmett, Ed.), Vol. 3, Chap. 3. Reinhold, New York, 1955.
2. I. M. Campbell, *in* "Catalysis at Surfaces," Chapman and Hall, London, 1988.
3. W. X. Pan, R. Cao, and G. L. Griffin, *J. Catal.* **114,** 447 (1988).
4. P. Courty, G. Durand, E. Freund, and A. Sugier, *J. Mol. Catal.* **17,** 241 (1982).
5. J. E. Baker, R. Burch, and S. E. Golunski, *Appl. Catal.* **53,** 279 (1989).
6. G. Fornasari, S. Gusi, F. Trifirò, and A. Vaccari, *Ind. Eng. Chem. Res.* **26,** 1501 (1987).
7. K. Klier, *Adv. Catal.* **31,** 243 (1982).
8. G. C. Chinchen, P. J. Denny, J. R. Jennings, M. S. Spencer, and K. C. Waugh, *Appl. Catal.* **36,** 1 (1988), and other references therein.
9. K. Klier, *Inorg. Chem.* **28,** 3868 (1989).
10. S. Metha, G. W. Simmons, K. Klier, and G. Hermann, *J. Catal.* **57,** 339 (1979).
11. C. Busetto, G. Del Piero, G. Manara, F. Trifirò, and A. Vaccari, *J. Catal.* **85,** 260 (1984).
12. W. Jones and M. Chibwe, *in* "Pillared Layered Structures" (I. V. Mitchell, Ed.), Chap. 2 Elsevier, London/New York, 1990.
13. S. Morpurgo, M. Lo Jacono, and P. Porta, *J. Mater. Chem.* **4,** 197 (1994).
14. X-Ray Powder Data File, ASTM cards: (a) 38-487 for hydrotalcite-like $Cu_2Zn_4Al_2(OH)_{16}CO_3 \cdot 4H_2O$; (b) 5-0661 for tenorite, CuO; (c) 36-1451 for zincite, ZnO; (d) 5-0669 for $ZnAl_2O_4$; (e) 33-448 for $CuAl_2O_4$; (f) 10-458 for $CoAl_2O_4$; (g) 23-1390 for $ZnCo_2O_4$; (h) 9-418 for Co_3O_4; (i) 4-836 for Cu^0.
15. S. J. Gurman, *in* "Applications of Synchrotron Radiation" (C. R. A. Catlow and G. N. Greaves, Eds.). Blackie, Glasgow, 1990.
16. R. Allman, *Acta Crystallogr.* **B24,** 972 (1968).
17. R. Allmann, *Chimia* **24,** 99 (1970).
18. P. Porta, S. De Rossi, G. Ferraris, M. Lo Jacono, G. Minelli, and G. Moretti, *J. Catal.* **109,** 367 (1988).
19. P. Porta, R. Dragone, G. Fierro, M. Inversi, M. Lo Jacono, and G. Moretti, *J. Mater. Chem.* **1**(4), 531 (1991).
20. H. Jaggi and H. R. Oswald, *Acta Crystallogr.* **14,** 1041 (1961).
21. R. D. Shannon, *Acta Crystallogr. Sect. A* **32,** 751 (1976).
22. N. M. D. Brown, J. B. McMonagle, and G. N. J. Greaves, *J. Chem. Soc. Faraday Trans. 1* **80,** 589 (1984).
23. M. Belli, A. Bianconi, S. Mobilio, L. Palladino, A. Reale, and E. Burattini, *Solid State Commun.* **35,** 355 (1988).
24. G. Vlaic, J. C. J. Bart, W. Cavigliolo, B. Pianzola, and S. Mobilio, *J. Catal.* **96,** 314 (1985).
25. G. Sankar, S. Vasudevan, and C. N. R. Rao, *J. Chem. Phys.* **85,** 2291 (1986).
26. K. Tohji, Udagawa, T. Mizushima, and A. Ueno, *J. Phys. Chem.* **89,** 5671 (1985).